

# THERMOPLASTIC TOWPREGS - AN INVESTIGATION OF THE HOT MELT PRODUCTION PROCESS

Prof. Dr. Ing. Thomas Gries; Max Schmidt, M.Sc.; Kai Cramer, M.Sc.  
Institut für Textiltechnik of RWTH Aachen University  
Aachen, Germany

## ABSTRACT

The impregnation of thermoplastic fiber composites usually requires heavy and expensive machinery. This still restricts the use of FKV in many areas. To reduce manufacturing costs, towpregs are used: they are of consistently high quality and require comparatively simple manufacturing steps.

In this paper a process developed at the Institute for Textile Technology for the production of thermoplastic towpregs is researched. In order to achieve the goal of a complete impregnation of the rovings a special tool was developed which serves as a basis for this paper. Due to the geometry of the tool, the carbon fibers are guided in a special way through the hot thermoplastic filled cavity. In order to control further parameters, a closed loop control for the roving guidance was developed and integrated into the machine.

In detailed process investigations the pull-off force, production speed and sizing were identified as primary process relevant parameters of the melt impregnation. Their influence was researched and evaluated. The impregnation tool produced in the course of the work has completely impregnated carbon fibers of different fineness with thermoplastic. Finally, the towpregs produced on laboratory scale were validated by evaluating optical and mechanical tests. The measurements show promising tensile strengths of the manufactured towpregs. These are in the range of the tensile strength of the fibers as stated by the manufacturer. First application tests show that they are suitable for winding processes or as a replacement for steel in ropes.

Keywords: Towpreg, Prepreg, Thermoplastic, Process  
Corresponding author:

## 1. INTRODUCTION

The process investigated in this paper is based on the mechanical spreading and fluid spreading of carbon fiber rovings. The fluid used here is a PA6 plastic melt, which is also used for impregnation and thus as a matrix material. The necessary spreading of the fibers and their impregnation is thus carried out in a single process step. Figure 1 shows a schematic diagram of the process used in this

paper.

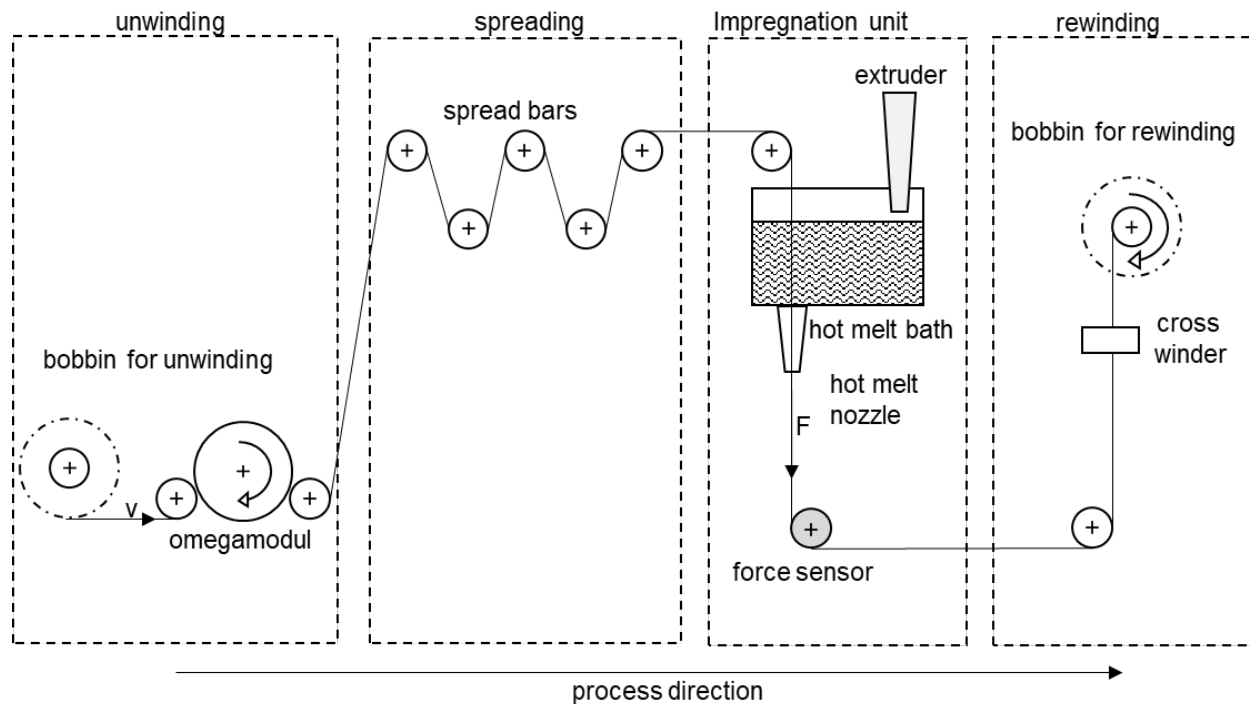


Figure 1: schematic view of the process

The process is divided into four sections. Unwinding by the omega module is used for controlled unwinding with a constant force within the process. In the second section, the fibers are pre-spread to break up the sizing and enable the impregnation of the fibers. The third section is for the actual impregnation. The impregnation process is completed at the hot melt nozzle. This is used to give the towpreg its final shape and fiber volume content. In the final section, the towpreg is wound back onto a spool by using a cross winder.

## 1.1 Parameters influencing the impregnation process

In the following, it will be explained which model is based on the process and which parameters have an influence on the towpreg.

### 1.1.1 Model conception: Darcy's law

The impregnation of a textile with a plastic can in principle be described with the model of the flow of an incompressible and viscous fluid through a homogeneous and porous material. Darcy's law gives a dependence of the averaged velocity  $v$  of the fluid relative to the porous material on the permeability  $K$ , the dynamic viscosity  $\eta$  and the gradient of the pore-averaged pressure  $\nabla p$  within the material. Darcy formulated a law as a special solution of the Navier-Stokes equation describing the impregnation as a one-dimensional flow [1]:

$$v = \frac{K}{\eta} \nabla p \quad (1.1)$$

The law assumes very slow flow velocities within the solid, so that the inertial forces of the fluid do not occur. Furthermore, this law only applies to flows with Reynolds numbers less than one. In addition, the fluid is considered a Newtonian fluid, so that its viscosity is independent of the shear rate  $\dot{\gamma}$ . Since the viscosity must remain constant, an isothermal process is also assumed. [2]

By integrating the equation, the required impregnation time  $\Delta t$  can be calculated, which is needed for the complete penetration of the fluid into the porous material [3]. The direction of  $z$  is orthogonal to the fibre towards the centre of the roving and has a quadratic effect on the required impregnation time.

$$\Delta t = \frac{\eta z^2}{2 K \Delta p} \quad (1.2)$$

To shorten the impregnation time at the same penetration depth in the  $z$ -direction, a reduction in viscosity or an increase in pressure is necessary. Since the viscosity, according to the assumption, remains constant and the permeability is an inherent variable, only the application of force can be favorably influenced.

### ***1.1.2 Permeability of the fiber***

In addition to the geometric dimensions, the modeling of the impregnation process also requires the determination of characteristic quantities of the two composite partners. A relevant technical quantity is the permeability  $K$ . It represents, as a constant tensor, the resistance of a porous medium against a penetrating flow of a fluid and is given in square millimeters. [2]

The degree of permeability of a porous material varies depending on the direction of injection and propagation. In principle, a distinction is made between one-dimensional flow, propagation in two dimensions on a plane, and three-dimensional flow through space [2]. It is a direction-dependent characteristic value of the fiber, which cannot be determined exactly [4].

For quantizing the permeability of a fiber, the Kozeny-Carman equation (see Equation 1.3) is used, which uses an empirical factor in an approximation. In this model, the property of the solid porous material within a single fiber bundle and between fibers is generally considered to be anisotropic. Here, the assumption is made that the individual fiber filaments are oriented in parallel and are uniformly distributed throughout the roving [5].

$$K = \frac{d_f^2 (1 - \varphi)^3}{k \varphi^2} \quad (1.3)$$

Using the fiber volume fraction  $\varphi$ , the filament diameter  $d_f$  and the Kozeny constant  $k$ , the Kozeny-Carman permeability is determined.

Further models extend the equation and include the anisotropy of the fiber [6]. The anisotropy results from the inhomogeneous distribution of the filaments and geometry changes of the roving. Usually, permeability can only be determined experimentally from measurements or, alternatively,

based on numerical methods. The latter methods require the determination of a large number of characteristic quantities which, in addition, are difficult to determine [5].

Based on the model of Kozney-Carmann, further models exist, which do not include an empirical factor. Furthermore, they consider the hexagonal or square arrangement of the fibers. According to [5], starting from the densest hexagonal packing, the permeability transverse and longitudinal to the fiber is calculated as follows:

$$K_{hex,\perp} = \frac{4}{9\pi\sqrt{6}} \left( \sqrt{\frac{\pi}{2\sqrt{3}\varphi}} - 1 \right)^{\frac{5}{2}} d_f^2 \quad (1.4)$$

$$K_{hex,\parallel} = \frac{2 d_f^2}{53} \frac{(1 - \varphi)^3}{\varphi^2} \quad (1.5)$$

Experimental methods use pressure measurement when indexing an air flow against a sample piece. In a benchmark study [1] in 2011, 16 different experimental methods for measuring the permeability of textiles were compared. It was shown that the values within a method remain approximately constant and are therefore reproducible. However, when the results of different methods for the same samples were compared, there was a deviation of a whole order of magnitude.

### ***1.1.3 Viscosity of the matrix***

The value of the dynamic viscosity  $\eta$  is required for the investigation of the impregnation behavior. Both temperature and shear rate influence the viscosity of thermoplastics.

Thermoplastics become lower viscosity when the shear rate is increased. This behavior is generally referred to as pseudoplastic or structural viscosity. Due to the very low shear rates used in this work, this effect can initially be neglected.

### ***1.1.4 Sizing of the fibers***

The preparation of the fiber has an influence on the machinability of the fiber and the subsequent fiber composite quality. Fiber filaments are coated by the manufacturer with a material on the surface called sizing. This provides interactions between the fibers and the matrix at the atomic level [7]. The filaments of a fiber are often inhomogeneously distributed. They are usually sized to improve fiber-matrix adhesion in thermoplastic composite applications [8]. Processing of a sized fiber is also easier because less fiber fly occurs and filament breaks are thus avoided.

Sizing is critical to the mechanical properties of a fiber-reinforced thermoplastic composite because the boundary between fiber and matrix is often the site of failure of a component. Especially when external forces are applied, good adhesion is necessary due to the low stiffness of the matrix. Thus, the transition from fiber to matrix represents the weakest point of the composite. From [9] it can be seen that thermoplastics partly show a better bonding to desized carbon fibers. However, the advantages of improved impregnation have to be weighed against the greater effort of processing unsized fibers.

### ***1.1.5 Spreading of the fiber material***

The spreading of fibers causes the individual filaments to expand and creates a larger surface area of the fiber, which has a positive effect on the impregnation process. A larger fiber bundle surface area statistically provides more opportunities for the plastic to penetrate the roving. At the same time, the spreading reduces the bundle diameter of the reinforcing fiber, so that the path of impregnation  $z$  becomes smaller. [8]

Technically, spreading can be mechanical or pneumatic. Mechanical spreading is realized by deflecting a drawn fiber with the aid of deflection rods.

### ***1.1.6 Other technically relevant physical parameters***

In addition to porosity, the quality of unidirectional tapes is mainly determined by morphological parameters such as the fiber volume content  $\varphi$ , fiber orientation, thickness of the matrix edge area, fiber corrugations, crystallinity and homogeneity of the fiber distribution [3].

The fiber volume content of a composite material is calculated from the ratio of the fiber volume  $V_f$  to the total volume, which is composed of the volume of the fiber and the volume of the matrix  $V_m$ .

$$\varphi = \frac{V_f}{V_f + V_m} \quad (1.6)$$

In particular, a homogeneous distribution of the fibers in the composite is crucial for the mechanical properties. The alignment in semi-finished products can no longer be changed in the subsequent finishing process, so that defects in the microstructure are systematically propagated in the course. Uneven fiber distribution leads to inhomogeneities, which in turn affect the permeability of the fiber.

A decrease in permeability also results in poorer impregnation quality. For this reason, a pre-spread homogeneous and parallel arrangement of the fibers is already of great importance when entering the melt impregnation process.

## 1.2 Design of the impregnation unit

The impregnation tool consists of a melt bath, the nozzle and the consolidating nozzle block. The assembly is shown in Figure 2 with a half-width cutaway view. The impregnation nozzle is mounted below the melting bath.

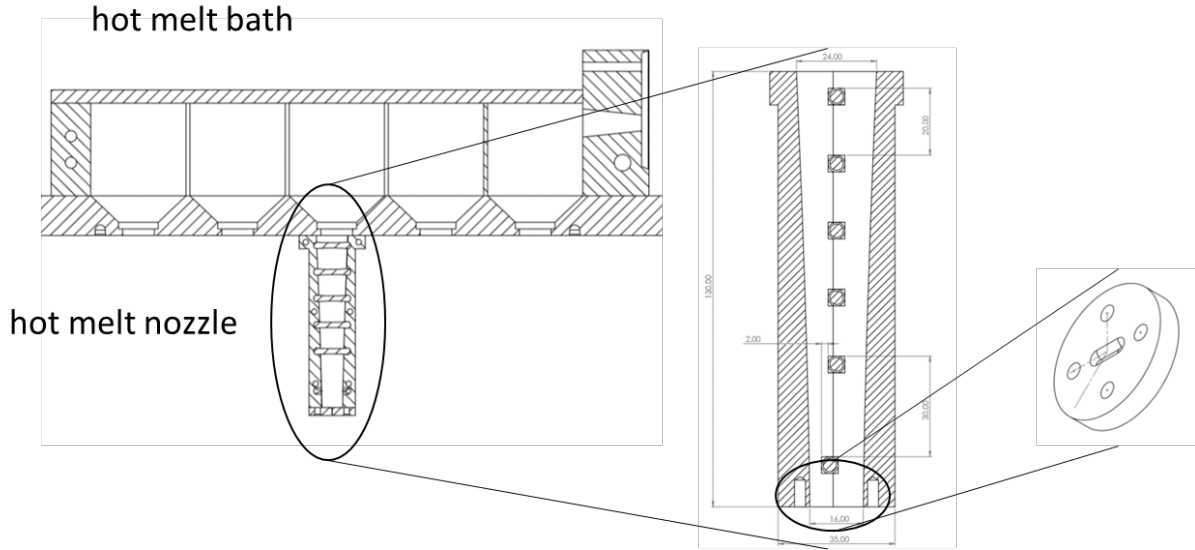


Figure 2: side view of the impregnation unit

The deflection bars integrated in the nozzle generate a force that results in the required impregnation pressure. An additional effect is the spreading of the fiber at the deflection bars. The polymer melted on the deflection rods gets between the filaments due to the shearing effect. As with spreading, the contact force of the fiber results from the product of the tensile stress  $F$  and the sine of the wrap angle  $\alpha$ . The wrap angle is a purely geometric quantity and, by equation 4.1, depends only on the diameter of the deflection  $d_U$  and the distance  $a$  in the  $x$ - and  $y$ -directions.

$$\alpha = 2 \left[ \arcsin \left( \frac{d_U}{\sqrt{a_x^2 + a_y^2}} \right) + \arctan \left( \frac{a_y}{a_x} \right) \right] \quad (1.7)$$

The larger the wrap angle, the greater the resulting force on the fiber and the associated positive effects of spreading and impregnation. According to the rope friction formula of Euler and Eytelwein, too large a wrap of the deflection generates too high friction [10]. Too high tension produces fiber damage and breakage of individual filaments up to the entire bundle.

For the designed nozzle, a wrap angle of  $\alpha = 23^\circ$  is targeted for one deflection. With a distance of  $a_x = 20 \text{ mm}$  at a deflection rod diameter  $d_U = 4.5 \text{ mm}$ , a wrap angle  $\alpha_1 = 23.07^\circ$  results (see equation 4.3).

$$\alpha_1 = 2 \left[ \arcsin \left( \frac{4 \text{ mm}}{\sqrt{20^2 \text{ mm}^2 + 0^2}} \right) + \arctan \left( \frac{0}{20} \right) \right] \approx 23.07^\circ \quad (1.8)$$

Since the roving is to leave the nozzle centered at the last deflection, the deflection is offset by  $a_y = 2$  mm, so that the distance between the last two deflections is adjusted to  $a_x = 30$  mm.

$$\alpha_2 = 2 \left[ \arcsin \left( \frac{4 \text{ mm}}{\sqrt{30^2 \text{ mm}^2 + 2^2 \text{ mm}^2}} \right) + \arctan \left( \frac{2}{30} \right) \right] \approx 22.92^\circ \quad (1.9)$$

The six deflections thus result in an added wrap angle of approximately 140 degrees. This wrap angle was found to be a practicable value based on the theoretical considerations in section 1.3 and preliminary tests.

After impregnation, the generated composite of fiber and plastic leaves the die through the die block, which adjusts the fiber volume content with its cross-section individually adapted to the fiber and determines the shape of the towpreg. Different nozzles are used depending on the desired geometry and the fiber volume content to be set.

Figure 3 shows an example of the nozzle head for the roving TENAX® ITS50 F23 from Teijin Carbon Europe GmbH, Wuppertal, which consists of 24,000 individual filaments. The nozzle head has a slot produced by an erosion process, which is rounded in the side facing the nozzle to prevent fiber damage. The slot has a cross-sectional area  $A_S = 1.431 \text{ mm}^2$  and the cross-sectional area of the fiber is  $A_F = 0.924 \text{ mm}^2$ . The theoretically achievable fiber volume content is  $\varphi = 63.15 \%$ . The wide slot consolidates the fiber composite to a thin and narrow towpreg, which has a tape-like cross-section.

### 1.3 Theoretical calculation of the process

For complete penetration of the roving, the process parameters are theoretically determined in this section. In the following, an exemplary calculation is carried out for a roving consisting of 24,000 single filaments with a filament diameter  $d_f = 7 \text{ }\mu\text{m}$ . The selected fiber has the largest diameter in this paper, so this calculation can be taken as the maximum limit of the design.

Equation (1.2) from Darcy's law can be used to determine the lower limit of the impregnation time required to completely impregnate the roving. It is valid as a function of viscosity, coordinate perpendicular to the fiber, permeability and pressure gradient.

The viscosity is assumed to be  $100 \text{ Pa}\cdot\text{s}$  from the data sheet of the plastic "BASF Ultramid® B24 N 03 - PA6". The depth to be impregnated is conservatively assumed to be half the diameter of the roving and is approximately  $0.54 \cdot 10^{-3} \text{ m}$  for a 24k roving. The permeability perpendicular to the fiber can be determined using Equation 1.4.

$$K_{\perp} = \frac{4}{9\pi\sqrt{6}} \left( \sqrt{\frac{\pi}{2\sqrt{3}\varphi}} - 1 \right)^{\frac{5}{2}} d_f^2 = \frac{4}{9\pi\sqrt{6}} \left( \sqrt{\frac{\pi}{2\sqrt{3} \cdot 0.45}} - 1 \right)^{\frac{5}{2}} (7 \cdot 10^{-6} \text{ m})^2 \approx 2.9 \cdot 10^{-12} \text{ m}^2 \quad (1.10)$$

The impregnation force  $F_S$  is a function of the tensile stress and the wrap angle. To calculate the impregnation force for an assumed tensile force of 100 N and a calculated wrap angle of  $23^\circ$  the resulting impregnation force  $F_S$  is:

$$F_S = F \cdot \sin(\alpha) = 100 \text{ N} \cdot \sin(23^\circ) \approx 39.07 \text{ N} \quad (1.11)$$

The pressure gradient results from the ratio of the force  $F_S$  to the contact area of the roving with the impregnation rod. The area is the product of the wrap angle, the diameter  $d_U$  of the impregnation rod and the spread width of the roving  $b_f$ .

$$\Delta p = \frac{F_S}{A} = \frac{F_S}{\frac{23}{360} \pi \cdot d_U \cdot b_f} = \frac{39.07 \text{ N}}{\frac{23}{360} \cdot \pi \cdot 4 \text{ mm} \cdot 2.5 \text{ mm}} = 19.465 \cdot 10^6 \text{ Pa} \quad (1.12)$$

With the determined data, a minimum impregnation time of

$$\Delta t = \frac{\eta z^2}{2 K \Delta p} = \frac{100 \text{ Pa s} \cdot (0.54 \cdot 10^{-3} \text{ m})^2}{2 \cdot 2.88 \cdot 10^{-12} \text{ m}^2 \cdot 19.465 \cdot 10^6 \text{ Pa}} = 0.612 \text{ s} \quad (1.13)$$

With this conservative calculation, an impregnation time of 0.612 seconds at a tensile stress of 100 N is required. The impregnation time describes the time in which the roving touches the impregnation rod. This in turn results in a maximum production speed  $v_{p,max}$  that can be set for the process, which is derived from the impregnation time and the length of the contact area  $l_k$  with six impregnation rods.

$$v_{p,max} = \frac{6 \cdot \frac{23}{360} \cdot \pi \cdot d_I}{\Delta t} = \frac{6 \cdot \frac{23}{360} \cdot \pi \cdot 0.004 \text{ m}}{0.612 \text{ s}} \approx 1,12 \frac{\text{m}}{\text{min}} \quad (1.14)$$

Thus, according to the present calculation, the maximum production speed of 1.12 m/min for a complete impregnation of a 24k fiber should not be exceeded. However, this calculation only takes into account the contact time of the fiber with the impregnation rods. Also, during the fiber conveying between the rods, the fiber is completely in the polymer melt, so the polymer penetrates the roving. Similarly, in this design, the permeability calculation was performed according to Equation (1.4), which calculates a fourfold order of magnitude lower permeability than the Carman-Kozeny equation.

## 2. EXPERIMENTATION

### 2.1 Materials

In order to evaluate the influence of different materials, a selection of fiber materials with different properties is made for the execution of the tests. The wide range of properties, such as sizing, sizing percentage, fiber density, fineness and strength, serves to improve the findings of the tests and determine dependencies.

The fiber materials used in this work are listed in Table 2.1. All fiber materials have a filament diameter  $d_f = 7 \mu\text{m}$ . The information of the number of filaments is included in the name of the respective fiber. In addition to the sizing percentage, the included sizing material is also noted in the column. The selection of the fibers used was made taking into account their compatibility with thermoplastic polymers. The exact designation of the sizing material used is subject to secrecy at the manufacturers, so that the specification of the materials of the sizing is only given in groups. To investigate the influence of the sizing on the impregnation process, an unsized fiber is also included in the test plan.

Table 2.1: Fiber materials used [11; 12]

Fiber	Fineness [tex]	Tensile strength $\sigma_f$ [MPa]	Young's modulus [GPa]	Density $\rho_f$ [g/cm <sup>3</sup> ]	Sizing [%]
Toho Tenax® E-HTA40 E13-6k	400	4100	240	1,77	1,3 EP
Mitsubishi Chemical Carbon 34-12K-R	1600	4830	234	1,8	unsized
Toho Tenax® E-UTS50-F24 24K	1600	5100	245	1,78	2,0 PU
Toho Tenax® E-ITS50-F23 24K	1600	5100	265	1,8	1,0 PU

The fiber "Mitsubishi Chemical Carbon 34-12K-R" could not be processed reliably and is therefore not considered further, but the test should be mentioned for the purpose of completeness.

The choice of matrix material is limited to the use of polyamide 6. Thus, the influence of the combination of fiber and plastic is limited. The properties of the plastic used are shown in Table 2.2. The polyamide 6 used from BASF SE, Ludwigshafen, is available as granules and has no additives that serve to stabilize the plastic or would influence the impregnation process.

Table 2.2: Properties of the plastic used thermoplastic [13]

Name	Melt temperature $T_s$ [°C]	Glas transition temperature $T_g$ [°C]	E-module [MPa]	density $\rho_m$ [g/cm <sup>3</sup> ]
BASF Ultramid® B24 N 03 - PA6	220	60	3500	1,14

## 2.2 Process parameters

The tests were carried out with different fibers, nozzles and process parameters. Table 2.3 shows the process-safe parameter ranges used in the tests. By process-safe it is meant here that the process ran stationary without disturbance.

Table 2.3: Parameter ranges of the test runs for stationary processes

Fiber	Process tension F [N]	Process speed $v_p$ [m/min]	Max. FVF [%]	Nozzle head
Tenax®-E HTA40-E13-6k	20 – 25 N	0,62 – 3,14	52,29	0.6 mm & 0.8 mm round
Tenax®-E UTS50-F24-24k	25 – 75 N	0,21 – 3,56	30,97	7 mm flat
Tenax®-E ITS50 F23 24K	25 – 75 N	0,21 – 2,72	31,12	7 mm flat

Figure 3 shows the nozzle heads used. The round 1 mm nozzle head is designed according to the 0.6 mm nozzle head, but with a correspondingly larger diameter.

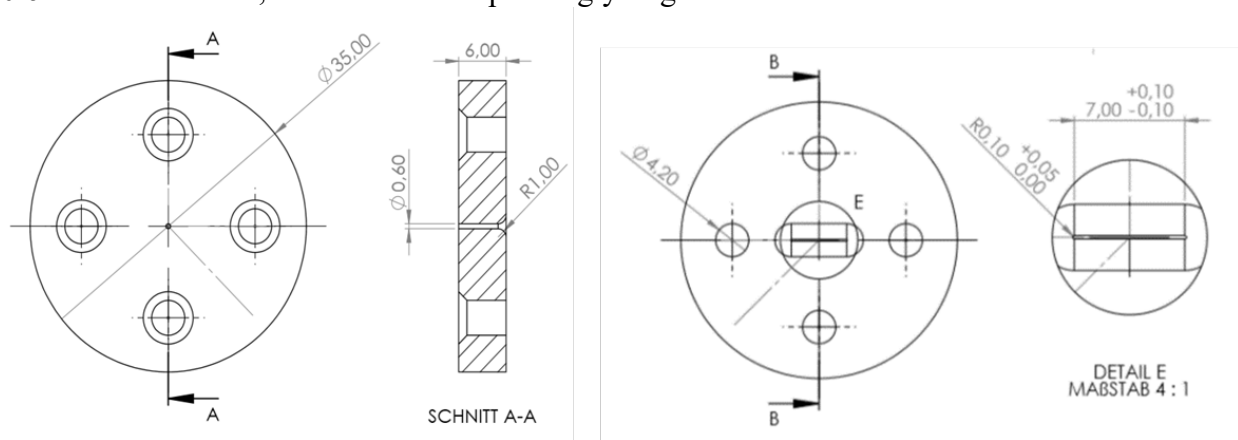


Figure 3: Nozzle heads; left 0.6 mm round, right 7 mm flat

### 3. RESULTS

In this chapter, the manufactured towpregs were tested and analyzed. Tensile tests and optical analyses are carried out and the fiber volume fraction is determined.

#### 3.1 Mechanical testing

The mechanical properties of the manufactured towpregs are of great importance, since thermoplastic fiber composites are used in structural components. Determination of the mechanical properties serves to evaluate the quality of the semi-finished product, so that conclusions can be drawn about damage to the structure if necessary. The experimental determination of tensile strength, Young's modulus and test specimen preparation is carried out according to DIN EN ISO 10618:2004 [14]. The results of the tensile tests of the fiber composites are shown below. The parameter sets are composed of the values of five specimens each.

Table 3.1: Tensile test results from Tenax®-E HTA40-E13-6k ( $\varphi = 52,10 \%$ ;  $A_v = 0,4338 \text{ mm}^2$ , 25 N process force, 1 m/min process speed)

Set of 5 specimen	F [N]	$\sigma$ [MPa]	E [GPa]
Average value $\bar{x}$	657,09	1514,73	134,7
Coefficient of variation $v$ [%]	6,36	6,36	7,74
Minimum value	609,76	1405,62	122,9
Maximum value	688,96	1588,20	142,8

Table 3.2: Tensile test results from Tenax®-E UTS50-F24-24k ( $\varphi = 29,00 \%$ ;  $A_v = 3,1172 \text{ mm}^2$ , 50 N process force, 1 m/min process speed)

Set of 5 specimen	F [N]	$\sigma$ [MPa]	E [GPa]
Average value $\bar{x}$	3263,49	1046,93	80,1
Coefficient of variation $v$ [%]	4,71	4,71	2,37
Minimum value	3069,88	984,82	78,5
Maximum value	3470,22	1113,25	83,2

Table 3.3: Tensile test results from Tenax®-E ITS50-F23-24k ( $\varphi = 30,96 \%$ ;  $A_v = 2,9199 \text{ mm}^2$ , 50 N process force, 1 m/min process speed)

Set of 5 specimen	F [N]	$\sigma$ [MPa]	E [GPa]
Average value $\bar{x}$	2872,74	983,85	81,8
Coefficient of variation $v$ [%]	5,04	5,04	4,2
Minimum value	2689,96	921,25	78,1
Maximum value	3091,27	1058,69	86,2

The measured results are compared with the calculated ones to validate the plausibility of the results. The coefficients of variation  $v$  are smaller than 10 % for all parameters, so that a statistically sufficient reliability of the values is assumed. In particular, the tests of the towpregs with 24,000 filaments show high confidence with coefficients of variation in the range of 5 %. Furthermore, the results of the tensile tests in Table 3.4 are compared with the values calculated from the data sheets.

Table 3.4: Comparison of tensile test measurements with calculated values

Fiber material	$F / F_{\max, f}$	$E / E_{\parallel, v}$
HTA40-E13-6k ( $\varphi = 50,23 \%$ )	$\frac{547,51 \text{ N}}{4100 \text{ MPa} \cdot 0,226 \text{ mm}^2} \hat{=} 59,09 \%$	$\frac{142,4 \text{ GPa}}{122,3 \text{ GPa}} \hat{=} 116,44 \%$

HTA40-E13-6k ( $\varphi = 52,10 \%$ )	$\frac{657,09 \text{ N}}{4100 \text{ MPa} \cdot 0,226 \text{ mm}^2} \cong 70,91 \%$	$\frac{134,7 \text{ GPa}}{126,7 \text{ GPa}} \cong 106,30 \%$
UTS50-F24-24k ( $\varphi = 29,00 \%$ )	$\frac{3263 \text{ N}}{5100 \text{ MPa} \cdot 0,904 \text{ mm}^2} \cong 70,78 \%$	$\frac{80,1 \text{ GPa}}{73,5 \text{ GPa}} \cong 108,93 \%$
ITS50-F23-24k ( $\varphi = 30,96 \%$ )	$\frac{2872 \text{ N}}{5100 \text{ MPa} \cdot 0,904 \text{ mm}^2} \cong 62,29 \%$	$\frac{81,8 \text{ GPa}}{84,46 \text{ GPa}} \cong 96,85 \%$

The measured elastic moduli are in a similar range of values as the calculated ones and have relative deviations in a range of 3.15 - 16.44 %, which are considered sufficient for the method. It is noticeable that the fiber volume fraction of the prepared specimens has a great influence on the elastic modulus.

The tensile stress values of the specimens correspond to 59 - 71 % of the values from the carbon fiber data sheets. On the one hand, this may be due to fiber breaks that occurred during impregnation, rewinding processes or spreading processes

In summary, the values determined can be assessed as statistically sufficient and plausible. The tensile strengths of the towpregs produced lie within a range of 59 - 71 % of the fiber manufacturers' specifications. The moduli of elasticity deviate by 3 - 16 % from the theoretically calculated values, so that it can be assumed that towpregs with predetermined properties can be produced reliably.

### 3.2 Influence of the production speed

Increasing the production speed influences the properties of the produced towpreg, so that the process parameter cannot be scaled without restrictions. It reduces the impregnation time and thus indirectly the degree of impregnation and the quality of the semi-finished product. According to Darcy's law, the fiber volume content increases by increasing the production speed. In addition, the process reliability of the impregnation line is influenced. In order to minimize the uncertainties due to other factors during the investigation, process parameters such as temperature, sizing, material usage and tensile stress are kept constant.

In the following, the dependence of the fiber volume content of towpregs made of Tenax®-E HTA40-E13-6k on the variation of the fiber speed is investigated. In Figure 4, two series of measurements of fiber volume content versus production speed are shown in a diagram. Each individual measured value represents the arithmetic mean of ten measurements. The first series of measurements was carried out using a nozzle with a 0.6 mm diameter and the second with a 0.8 mm diameter.

The first series of measurements was performed using a nozzle stone with a round outlet diameter of 0.8 mm, resulting in a fiber composite with an average fiber volume content of 33%. A round nozzle die with a diameter of 0.6 mm was used for the second series of measurements. This resulted in fiber volume contents above 50 %.

Both semifinished products obtained a higher fiber volume content with increasing production speed. A general functional dependence cannot be exactly determined on the basis of the different slopes. While the interpolated function of the first measurement shows a steeper increase, the regression curve of the first measurement is relatively flat.

The impregnation with a low fiber volume content has a higher influenceability by the production speed than fiber composites with a higher fiber content. At production speeds of 0.62 - 1.23 m/min, the fiber volume content of 0.6 mm nozzle increases by only 2.5 volume percent. The fiber volume content of the 0.8 mm nozzle increases by 7.5 volume percent.

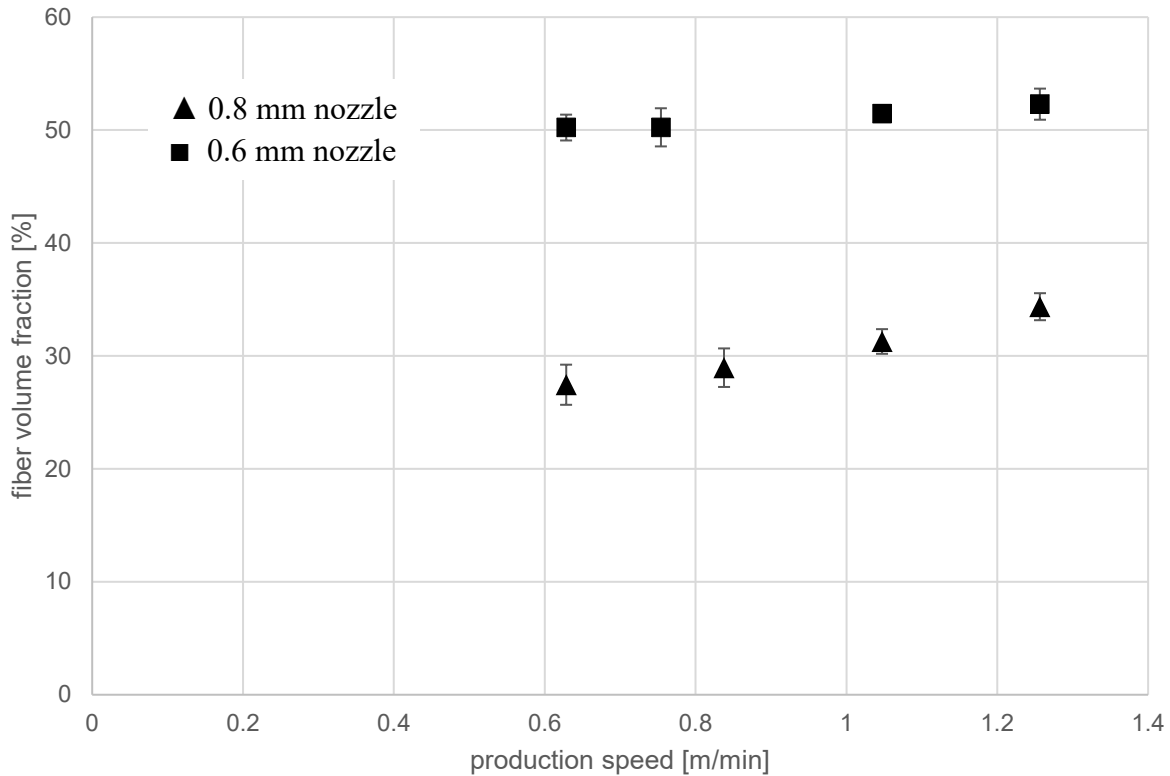
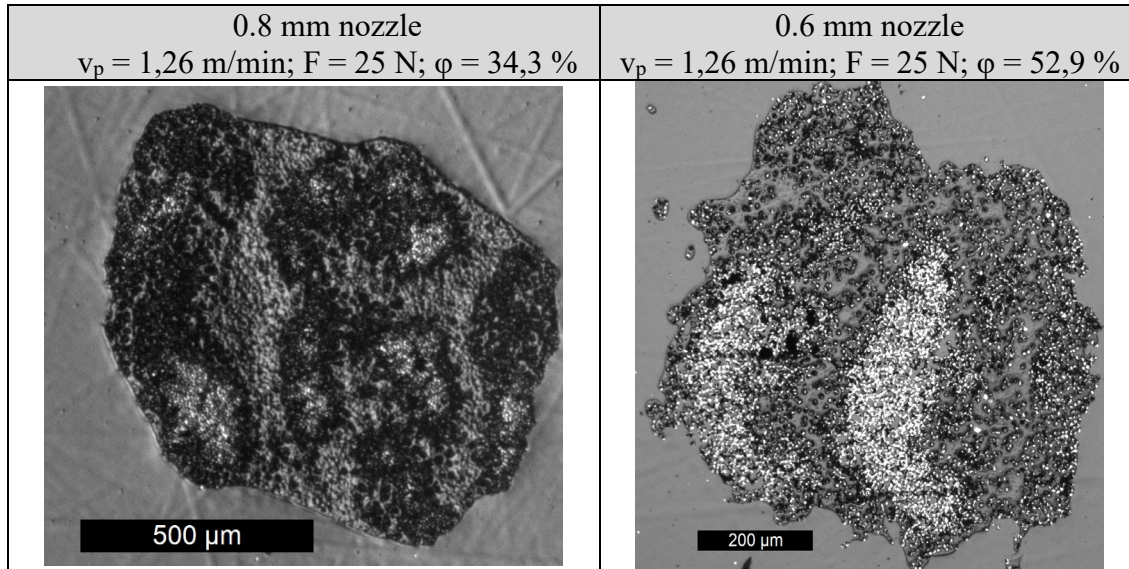


Figure 4: Fiber volume fraction as a function of the production speed of two series of measurements of towpregs made of Tenax®-E HTA40-E13-6k

Increasing the production speed results in a reduction of the impregnation time in the same ratio. Based on the results obtained, an almost linear relationship between production speed and fiber volume fraction can be assumed. Microscopy images of the semi-finished products of both series of measurements are shown in Table 3.5. The micrographs were taken from towpregs produced at the highest production speed. On both images it can be seen that the roving was completely penetrated by the matrix. Furthermore, no damage or cracks can be seen in the cross-section of the towpreg, so that the speeds achieved do not have a limiting effect on the process. The filaments have an almost homogeneous structure.

Table 3.5: microscopy view of the semifinished product made of Tenax®-E HTA40-E13-6k  
(Parameter:  $v_p = 1,26$  m/min;  $F = 25$  N).



The assumption made of increasing the fiber volume fraction could be verified for the thermoplastic impregnation of Tenax®-E HTA40-E13-6k. An increase in the production speed results in a reduction in the impregnation time, so that higher proportions of the fiber are present in the composite. Round semi-finished product geometries were produced during the trials.

### 3.3 Influence of the process tension

The control of the tension of the fiber in the process is done continuously by the take-up and sets the pressure difference  $\Delta p$  required for impregnation. According to Darcy's law, the achievable depth of impregnation  $z$  increases with increasing pressure, so that high tensile forces favor the process of impregnation.

In the process, the fiber is spread and impregnated by rods made of steel. A high tension along the fiber results in high friction. These causes filament breaks and negative semi-finished product quality. Consequently, the maximum tension should be adjusted so that the fiber is completely impregnated by the polymer during impregnation and at the same time little fiber damage occurs. The diagram shown in Figure 5 shows the influence of the tension on the fiber volume fraction of a manufactured towpreg made of Tenax®-E ITS50-F23-24k at a constant production speed of 1.05 m/min. To overcome the holding forces on the impregnation and rods, a force of about 25 N is required for the roving of 24,000 filaments to ensure continuous conveying. Forces below 25 N cannot overcome the holding forces of the rods and spreading bars, so that the fiber is not moved. Above this threshold, the graph shows no significant influence on the fiber volume fraction.

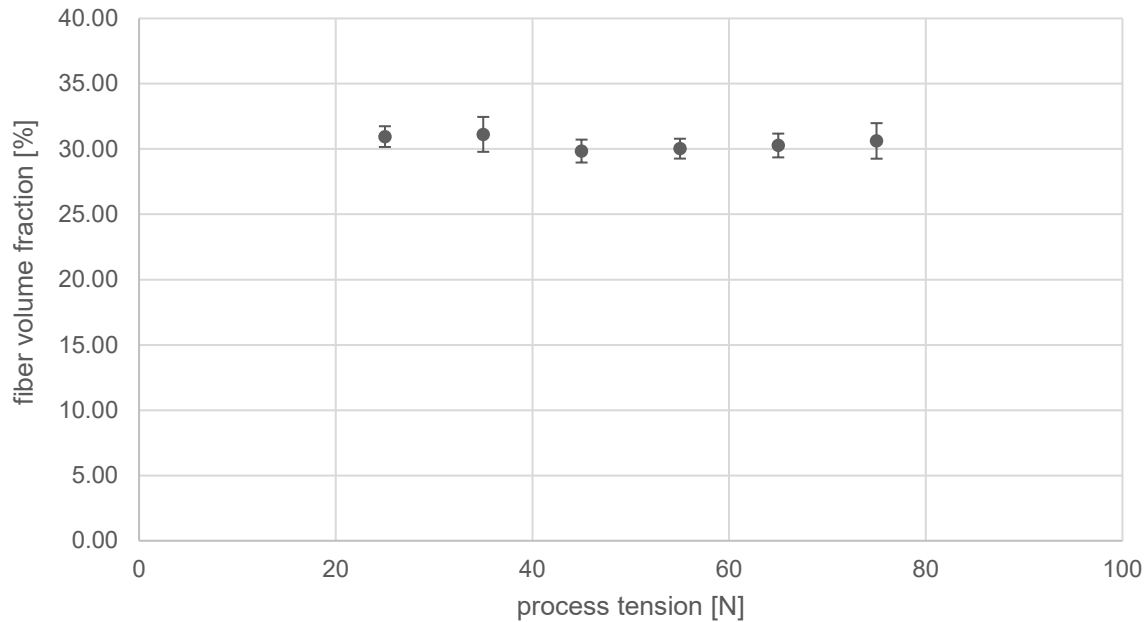


Figure 5: Fiber volume fraction as a function of the tensile strength of the impregnation of Tenax®-E ITS50-F23-24k (parameter:  $v_p = 1,05 \text{ m/min}$ )

One possible cause of the progression is the high friction on the spreading bars in front of the die. The tensile stress on the roving required to overcome the holding forces is already sufficient to achieve complete penetration of the carbon fiber in the die. An assumed high fiber volume content, due to incomplete penetration of the polymer in the lower range of the tensile force, is therefore not achieved.

The evaluations of prepared tensile specimens from towpregs impregnated with different tensile forces are used to examine for possible fiber breaks (see Figure 6). Five specimens were prepared, each for one investigated point of the fiber tensile force.

The curves of the tensile forces basically show a similar behavior. Noticeable are the high statistical uncertainties in the range of low fiber tensile forces, which can be seen in the error bars. For example, the measurement series of ITS50 has a coefficient of variation of 20 in the second measurement point. The series of measurements in the range of fiber tensile forces of 25 - 35 N each have an outlier, which affects the statistical confidence and reduces the mean values of the maximum tensile forces of the fiber composites. Excluding the outliers in the evaluation would result in a maximum tensile force of 3000 N, which would remain constant over all fiber tensile forces.

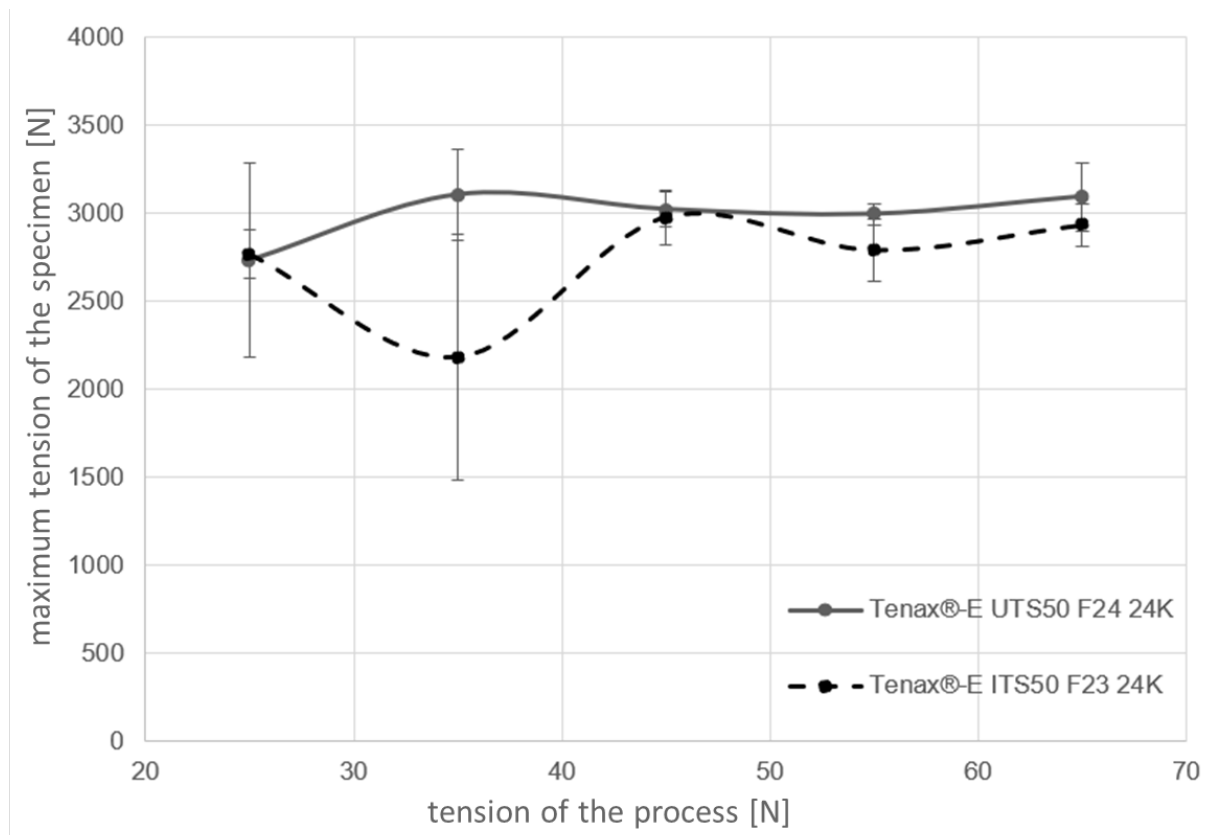


Figure 6: Maximum tensile force of the towpregs as a function of the tensile force of the process of Tenax®-E ITS50-F23-24k and Tenax®-E UTS50-F24-24k

The examination of the tensile specimens shows no significant changes in the maximum tensile forces at higher fiber tensile forces. Only a high process uncertainty in the lower fiber tension range can be observed. This can be explained by the fact that the measured values of the lower range were generated shortly after start-up and thus took place earlier in the process. A melt that is not yet homogeneous can damage the fibers and create defects. The exponentially interpolated lines of the measuring points shown can also be interpolated linearly. A precise determination is not possible. Nevertheless, a tendency for the trend lines to increase slightly with increasing fiber tensile strength is indicated. To a first approximation, the fiber tensile force has only a minimal influence on the achievable tensile forces and thus on the fiber damage in the process.

### 3.4 Influence of the sizing

Manufacturers offer carbon fibers with different sizing materials. Based on the choice of plastic for the desired FRP, a suitable sizing can be selected. Preparing the fiber with a sizing additionally enables improved processability. It allows the filaments to adhere to each other and prevents fiber breakage due to fiber separation, which is generated electrostatically or by excessive humidity, for example.

The fiber type Tenax®-E HTA40-E13-6k, with an epoxy sizing of 1.3%, was increasingly used in this work for the production of towpregs. To further investigate the influence of its sizing, a thermal process was used to desize the roving and compare it with the untreated fiber.

In the desizing process, the roving is unwound and conveyed through an oven that evaporates the epoxy size at 600 °C under inert gas. Subsequently, the desized fibers are rewound so that they can be loaded into the impregnation plant. Weighing of the desized filament showed a weight loss of 5 tex. As a result, the desized fiber has a new fineness of 395 tex. This value corresponds to the 5.2 tex sizing percentage specified by the manufacturer, so that a successful complete desizing process is assumed. The comparison of the fibers is made by plotting the fiber volume fraction versus production speed in Figure 7. Shown are trials of the untreated sized fiber and of the desized fiber.

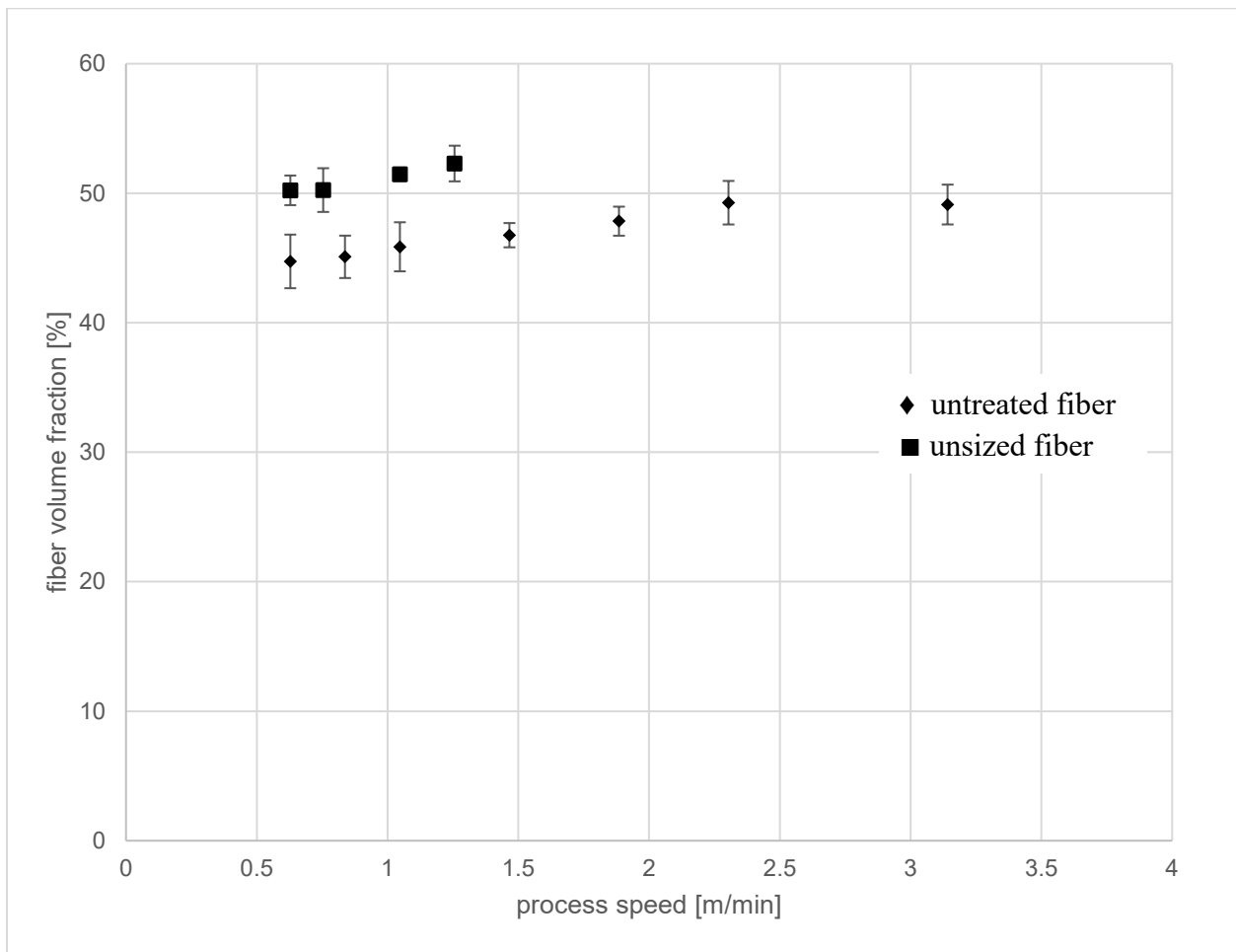


Figure 7: Diagram visualizing the influence of the sizing on the fiber volume fraction via the production speed

As already noted, an increase in fiber volume fraction with increasing production speed can be seen, which is also confirmed for unsized fibers. High process speeds are not possible with unsized fibers and lead to breaking of the roving.

The different fiber volume fractions cause deposits of fibers in front of the die and influence the process carried out. The increase of the fiber volume content change is approximately the same in all investigations, so that a similar behavior of the impregnation can be assumed.

When the test is carried out with the unsized fiber, increased filament breaks occur. In addition, fiber residues remain in the die, so that increased fiber breakage is assumed. Despite this, this unsized fiber could be impregnated without a process break.

In addition, tests of impregnation of an unsized carbon fiber provided by the manufacturer were undertaken. Three trials were carried out with the fiber 34-15k R with 0.0% U from Mitsubishi Chemical Europe GmbH, Düsseldorf, which all ended after a short time with a fiber break in the nozzle and could not be processed.

Since the trials of the unsized fiber show similar behavior to the fibers with sizing, the use of carbon fiber rovings with size is recommended for future trials. Preparation with size offers the advantages of easy handling during scaffolding, higher process reliability and less fiber breakage at the spreading bars and deflections.

#### 4. CONCLUSIONS

In the course of numerous tests, fiber volume contents of up to 52% could be achieved. Mechanical tensile tests have shown a tensile strength of 70% of the fiber strengths of the manufacturer's specifications, which can be attributed to fiber damage in the process. Furthermore, elastic moduli in the range of the manufacturer's specifications could be achieved.

By specifying the geometry of nozzle openings, it was possible to successfully adjust the cross-section of the fiber-reinforced composites produced. Round profiles with a diameter of 0.6 mm or 1 mm and flat profiles with cross-sectional dimensions of 0.6 x 7 mm<sup>2</sup> could be produced. The modularly exchangeable die stones also successfully influenced the fiber volume content. Precise adjustment of the fiber content was not possible, but could be reproduced. It was found that both the ratio of the nozzle opening to the fiber cross-section and the nozzle head geometry have a significant influence on the fiber volume content of the semi-finished product.

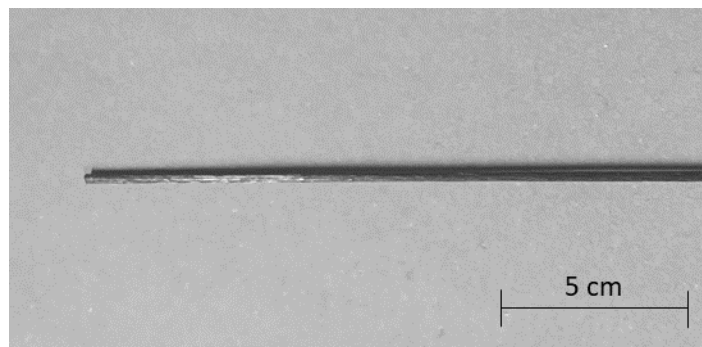


Figure 8: Produced towpreg with a cross section of 0.6 mm ( $\varphi = 52\%$ )

Qualitative evaluations of optical microscopy images and quantitative investigations of tensile tests have shown influencing parameters for the production of the semi-finished product, which result from the interplay of production speed, fiber force, fiber sizing and the fiber. The use of both thermally desized fibers and unsized fibers has shown no influence on the fiber volume content of manufactured towpregs. The use of desized fibers has only resulted in process uncertainty due to

fiber breakage and equipment setup difficulties. Increasing production speed has resulted in a decrease in matrix volume fraction, limiting the scaling of the process. An effect of fiber tensile strength on fiber volume content or strength could not be confirmed. However, improvements in impregnation quality were observed by light microscopy images.

For subsequent investigations, further nozzle bricks were constructed, which should achieve higher fiber volume contents in further tests. For the investigation of the processes at the nozzle head, a fluid simulation is also useful in order to better investigate the flow processes of the melt. The development of an in-process adjustment of the nozzle outlet cross-section represents a further approach to setting higher fiber volume contents. The focus here should not only be on the ratio of fiber cross-section to die outlet area, but also on the influence of die outlet area to circumference on the fiber volume content and the homogeneity of the fiber distribution.

## 5. REFERENCES

- [1] Arbter R, Beraud JM, Binetruy C, Bizet L, Bréard J, Comas-Cardona S, et al., Experimental determination of the permeability of textiles: A benchmark exercise, In „Composites Part A: Applied Science and Manufacturing“, p. 1157–1168, 9, 2011 [10.1016/j.compositesa.2011.04.021]
- [2] Nunes, J. P.; van Hattum, F. W. J.; Bernardo, C. A.; Silva, J. F.; Marques, A. T.: Advances in Thermoplastic Matrix Towpregs Processing, In „Journal of Thermoplastic Composite Materials“, p. 523–544, 6, 2004 [10.1177/0892705704038470]
- [3] Hopmann, Christian; Wilms, Erik; Beste, Christian; Schneider, Daniel; Fischer, Kai; Stender, Sebastian, Investigation of the influence of melt-impregnation parameters on the morphology of thermoplastic UD-tapes and a method for quantifying the same, In “Journal of Thermoplastic Composite Materials”, p. 1530-7980, 14, 2019. [10.1177/0892705719864624]
- [4] Luisier, A.; Bourban, P.-E.; Månson, J.-A.E.: Reaction injection pultrusion of PA12 composites: process and modelling, In „Composites Part A: Applied Science and Manufacturing“, p. 283-595, 7, 2003 [10.1016/S1359-835X(03)00101-5]
- [5] Gebart, B. R.: Permeability of Unidirectional Reinforcements for RTM, In „Journal of Composite Materials“, p. 1100-1133, 8, 1992. [10.1177/002199839202600802]
- [6] Gutowski, T. G.; Cai, Z.; Bauer, S.; Boucher, D.; Kingery, J.; Wineman, S.: Consolidation Experiments for Laminate Composites, In „Journal of Composite Materials“, p. 650-669, 7, 1987 [10.1177/002199838702100705]
- [7] Cherif, Chokri: Textile Werkstoffe für den Leichtbau, Berlin: Springer Verlag, 2011
- [8] Connor, Marco Tom: Consolidation mechanisms and interfacial phenomena in thermoplastic powder impregnated composites, Lausanne, EPFL, 1995

- [9] Hogg, P.J.; Ahmadnia, A.; Guild, F.J., The mechanical properties of non-crimped fabric-based composites, In „Composites“, S. 423-432, 5, 1993 [10.1016/0010-4361(93)90249-8]
- [10] Popov, Valentin L.: Kontaktmechanik und Reibung, Berlin, Heidelberg: Springer Berlin Heidelberg, 2010
- [11] Toray Composite Materials America, Inc.: Technical datasheet TORAYCA®
- [12] Mitsubishi chemical carbon fiber and composites, Inc.: Technical datasheet PAN fiber
- [13] BASF SE: Technical datasheet BASF Ultramid® Polyamide
- [14] DIN EN ISO 10618 (November 2004). Kohlenstofffasern – Bestimmung des Zugverhaltens von harz imprägnierten Garnen